

## Relativistic Mean Field Theory for Hypernuclei<sup>\*</sup>

NING Ping-Zhi<sup>1)</sup> TAN Yu-Hong LI Lei LUO Yan-An

(Department of Physics, Nankai University, Tianjin 300071, China)

**Abstract** The results of relativistic mean field (RMF) calculations are presented for some of strange, charmed and bottom hypernuclei and compared to each other. The calculation includes single particle energies and other static properties of hypernuclei with different flavours. The potential well depths and coupling constants of these flavoured baryons are estimated and the results show rich behaviour. A search for charmed hypernucleus with atomic number  $A \geq 100$  is suggested. Possible influences of different baryons impurities on the core nucleus are also examined.

**Key words** flavoured nuclei, heavy baryon-nucleus potential, single-particle spectra, relativistic mean field model

### 1 Introduction

The study of hypernuclei is of great scientific interest, it gives indeed a new dimension to the traditional world of nuclei by revealing the existence of a new type of nuclear matter. It contains baryon with strange  $S$ , namely,  $\Lambda$ -hyperon ( $S = -1$ ),  $\Sigma$ -hyperon ( $S = -1$ ),  $\Xi$ -hyperon ( $S = -2$ ) and so on. A large number of  $\Lambda$ -hypernuclei have been observed and systematic studies for these  $\Lambda$  hypernuclei known at present have provided the binding energies  $B$  of the  $\Lambda$ -single particle states in nuclei<sup>[1-3]</sup>.  $B$  varies linearly with mass number  $A$  with a slope of about 1 MeV/(unit of  $A$ ) and saturates at about 23 MeV for the heavy hypernuclei. This behavior suggests a simple model in which the  $\Lambda$  particle is confined in a potential well with a radius equal to the nuclear radius. The potential well depth may extract from these binding energy data, and much of what we know of the  $\Lambda N$  interaction comes from studies of the  $\Lambda$ -nucleus potential. Comparing with the  $\Lambda$ -hypernuclei, we know very few to other hypernuclei. Moreover, a recent experiment gives the negative answer on the existence of  $\Sigma$ -hypernuclei<sup>[4]</sup>. This kind of situation is stimulating more theoretical efforts and experimental measurements to understand the physics of hypernuclei.

On the other hand, it is generally agreed that hypernu-

clei represent the first kind of flavoured nuclei (with new quantum numbers), in the direction of other exotic nuclear systems, such as charmed and bottom hypernuclei. In fact, soon after the discovery of charmed particles  $\Lambda_c$ , it had been suggested that, in analogy with the strange nuclei, there should also exist the charmed nuclei<sup>[5-8]</sup>.

The  $\Lambda_c$ -nucleus potential describes the behavior of a charmed baryon  $\Lambda_c$  in the nuclear medium. Early works for charmed hypernuclei achieved different estimates about the binding energy and the potential well depth. Dover and Kahana<sup>[5]</sup> proposed that "the  $\Lambda_c$ -nucleus potentials are seen to be comparable in depth to the nucleon-nucleus potential". Batusov et al.<sup>[8]</sup> advanced that the binding energy of a charmed baryon  $\Lambda_c$  seems to be as large as that of  $\Lambda$  in hypernuclei. Band  $\bar{o}$  and Nagata<sup>[6]</sup> made a theoretical estimate of  $\Lambda_c$  hypernuclei and the calculated potential depth for  $\Lambda_c$  is 2/3 of that for  $\Lambda$ . Up to now, the  $\Lambda_c$ -nucleus potential is still unclear because the experimental information on the potential is absent. However, from the existing experimental data, indeed there are some signs expressing the existence of  $\Lambda_c$  hypernuclei<sup>[8-10]</sup>. Now, in the Japan Hadron Facility (JHF), the experiment to search for the charmed and the bottom hypernuclei ( $\Lambda_c$ -,  $\Lambda_b$ - hypernuclei) is becoming realistic. Careful estimates of the possible bound states of such

Received 29 November 2003, Revised 29 March 2004

\* Supported by National Natural Science Foundation of China (10275037) and Special Research Fund for Doctoral Program of Higher Education of China (20010055012)

1) E-mail: ningpz@nankai.edu.cn

exotic nuclei are needed.

In this work, we study some of strange, charmed and bottom hypernuclei within the framework of the RMF model. Our aim is to examine their potential well depths and single particle energies. Due to a hyperon behaves as an impurity in nuclei, we also consider the additions of the different baryons to some closed-shell nuclei and observe the influence of different baryons impurities on the core nucleus.

The RMF model used in our calculations is described in the following section. In Sec.3 we present results of the calculations. The summary and conclusions are drawn in Sec. 4.

## 2 The model

Because the relativistic mean-field model is a very standard theory that have been widely used to describe finite nuclei, nuclear matter and hypernuclei, all the formulations and the methods of numerical calculations have been clearly given in Refs.[11—15]. Here we only make a short description on the inputs in our calculations.

For the nucleonic sector, the NL-SH force parameters by Sharma et al.<sup>[12]</sup> are used in the calculation. In the case of the hyperons and the heavy flavored baryons, labeled as

$$Y = \Lambda, \Xi^-, \Xi^0, \Lambda_c^+, \Lambda_b, \Xi_c^+, \text{ or } \Xi_c^0,$$

Lagrangian density

$$L_Y = \bar{\psi}_Y (i\gamma^\mu \partial_\mu - m_Y - g_{\sigma Y} \sigma - g_{\omega Y} \gamma^0 \omega_0 - \frac{1}{2} g_{\rho Y} \gamma^0 \tau_{3,Y} \rho^0 - e\gamma^0 Q_Y A_0) \psi_Y. \quad (1)$$

is used to describe the flavored baryon and its couplings to the  $\sigma$ -,  $\omega$ -, and  $\rho$ -meson fields, where  $eQ_Y$  is the electric charge of the hyperons. The  $\Lambda$ ,  $\Lambda_c^+$  and  $\Lambda_b$  are isoscalar baryons which have isospin and charge zero and therefore cannot couple to the  $\rho$ -meson field and the electromagnetic field. To properly describe the properties of  $\Lambda$  hypernuclei, parametrization about  $\Lambda$  hyperon is taken from Ref. [13], where a tensor coupling term  $+ f_{\omega\Lambda} \bar{\psi}_\Lambda \sigma^{i0} \partial_i \omega_0 \psi_\Lambda / 2m_Y$  of vector meson is also included, here  $\sigma^{i0} = (i/2) \{ \gamma^i, \gamma^0 \}$ ,  $i = 1, 2, 3$ .

With a quark model approximation<sup>[16]</sup> that the light unflavored ( $S = C = B = 0$ ) meson fields couple to u, d quarks only, coupling constants of hyperons to the vector meson fields have the following quantitative relations

$$\frac{1}{3} g_{\omega N} = g_{\omega \Xi^-} = g_{\omega \Xi^0} = g_{\omega \Xi_c^+},$$

$$g_{\rho N} = g_{\rho \Xi^-} = g_{\rho \Xi^0} = g_{\rho \Xi_c^+},$$

$$\frac{2}{3} g_{\omega N} = g_{\omega \Lambda} = g_{\omega \Lambda_c^+} = g_{\omega \Lambda_b}. \quad (2)$$

The coupling constants to the scalar meson fields can be determined by the experimental information—the optical potential. It turns out that the scalar and the vector coupling constants of a hyperon are strongly correlated to its depth of the potential well in saturation nuclear matter<sup>[17,18]</sup>

$$U_Y = g_{\sigma Y} \sigma^{eq} + g_{\omega Y} \omega_0^{eq}. \quad (3)$$

Using these parametrization of RMF theory, one can make quantitative stus on various properties of hypernuclei, such as the singleparticle energy levels, binding energy per baryon, r. m. s. radii of baryons distributions, etc.

## 3 Results of calculations

It is well known that the potential well depth of  $\Lambda$  hyperon in nuclear matter is about  $-30\text{MeV}$ , so we can choose  $U_Y = -30\text{MeV}$  to obtain the coupling constant  $g_{\sigma\Lambda}$ . Then all the field equations are solved self-consistently in the mean filed approximation for finite nuclei. The calculated  $\Lambda$  singleparticle energies are in good agreement with the experiments<sup>[19]</sup>, and the observed very small spinorbit splitting for  $\Lambda$  hypernuclei is also consistent with the earlier phenomenological analysis.

However, experimental data on  $\Xi$  hypernuclei are very little, and, there is even no experimental data available on  $\Lambda_c^+$ ,  $\Lambda_b$ ,  $\Xi_c^+$  and  $\Xi_c^0$  yet, their depth of  $U_Y$  in nuclear matter is not known. Dover et al.<sup>[5]</sup> estimated that the  $\Lambda_c^+$ -nucleus potential is comparable in depth to the nucleon-nucleus potential, while Bando et al.<sup>[6]</sup> suggested  $U_{\Lambda_c^+}/U_\Lambda \approx 2/3$  and  $U_{\Lambda_b}/U_\Lambda \approx 1$  within the framework of the lowest-order Brueckner theory by employing the OBE potentials derived from the Nijmegen model. D. Starkov et al.<sup>[20]</sup> reported that, roughly,  $V_{\Lambda_c^+ N}(r) \approx kV_{\Lambda N}(r)$ ,  $k \approx 0.8$ , where  $V_{\Lambda_c^+ N}$  and  $V_{\Lambda N}$  are  $\Lambda_c^+$ -N and  $\Lambda$ -N potential, respectively. The value of  $k$  is intermediate between 1 as reported by Rufa et al.<sup>[21]</sup> and 0.5 as assumed by Tan et al.<sup>[19]</sup> and Shen et al.<sup>[22]</sup> on the basis of the  $2\pi$ -exchange alone.  $\Lambda_c^+$  has a positive electric charge, whereas  $\Lambda$  or  $\Lambda_b$  is neutral, therefore, the Coulomb effects may play a non-negligible role in hypernuclei. On the other hand, the large mass of  $\Lambda_c^+$  and  $\Lambda_b$  means that it may be more strongly bound than  $\Lambda$ .

To investigate the effects of various values of hyperon-nucleus potential  $U_Y$ , we actually choose  $U_Y = -40, -30,$

**Table 1. Hyperon single-particle energies (in MeV) in core nucleus  $^{16}\text{O}$ .**

	$^{16}\Lambda\text{O}(\text{exp})$	$^{17}\Lambda\text{O}$	$^{17}\Lambda_c^+\text{F}$			$^{17}\Lambda_b^+\text{O}$			
			-40	-30	-20	-40	-30	-20	-10
$1s_{1/2}$	-12.5	-12.3	-23.3	-13.0	-4.91	-35.9	-22.4	-12.1	-5.1
$1p_{3/2}$	-2.5	-2.5	-13.9	-6.4	-0.9	-28.6	-18.0	-9.5	-3.9
$1p_{1/2}$	(1p)	-2.2	-13.4	-6.0	-0.6	-28.5	-17.9	-9.4	-3.8
$1d_{5/2}$			-5.2	-0.1		-22.2	-13.3	-6.5	-2.2
$2s_{1/2}$			-4.5			-20.9	-12.5	-5.8	-0.6
$1d_{3/2}$			-4.4			-22.0	-13.2	-6.4	-2.2
$1f_{7/2}$						-16.0	-8.7	-3.4	-0.3

-20, -10MeV for  $\Lambda_c^+$  and  $\Lambda_b$ , compare the results of the single-particle energies in core nuclei  $^{16}\text{O}$ ,  $^{90}\text{Zr}$  and  $^{208}\text{Pb}$ , which is respectively presented in Tables 1, 2, 3. The results for  $\Lambda$  hyperon in the corresponding nuclei are also given as comparison. The experimental data are taken from Refs. [24,25]. It can be seen that  $\Lambda_c^+$  would not bind to any of these three nuclei if  $\Lambda_c^+$  potential well depth in nuclear matter is less than 10MeV. When  $U_{\Lambda_c^+} = -20\text{MeV}$ , it begins to bind to  $^{16}\text{O}$  and  $^{90}\text{Zr}$ , but not yet to  $^{208}\text{Pb}$ , while  $\Lambda_b$  can bind to all of the three nuclei with  $U_{\Lambda_b}$  ranging from -40MeV to -10MeV. It can also be seen that, the change of potential well depth will result in a large movement for the single-particle energies. When  $U_Y$  goes deeper, the single-particle energies of  $\Lambda_c^+$  or  $\Lambda_b$  increases significantly. We can conclude that the repulsive Coulomb interaction between the  $\Lambda_c^+$  and protons leads a considerable lowering to the binding energy of  $\Lambda_c^+$  in nuclei. Besides, a small spin-orbit splitting of  $\Lambda$ - and  $\Lambda_c^+$ -hypernuclei is also observed, while the similar splitting for  $\Lambda_b$ -hypernuclei is almost zero. A small level spacing of  $\Lambda_b$  single-particle energies has been obtained and compared with those of  $\Lambda$  and  $\Lambda_c^+$ . Just as the suggestion by Tsushima et al. [16], this may be a consequence of the heavier mass, and

the small level spacing would make much more difficulties to distinguish the states in an experiment, or imply some new phenomena. The results of  $\Lambda_c^+$  and  $\Lambda_b$  single-particle energies in Ref. [16] are very close to ours at the value of  $U_Y = -30\text{MeV}$ .

Now we make a brief discussion on theoretical results of  $\Lambda_c^+$  hypernuclei systematically. The  $1s_{1/2}$   $\Lambda_c^+$  binding energies as a function of atomic numbers are given in Fig. 1, where the proton numbers are set to be equal to the neutron number for all the nuclides. The solid and dashed lines

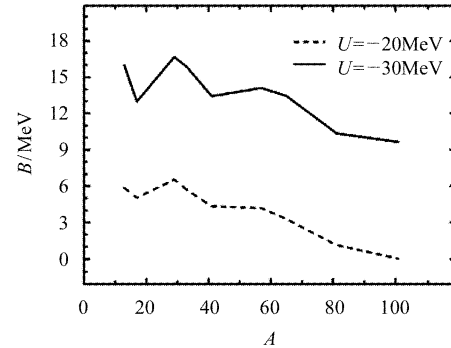


Fig. 1.  $\Lambda_c^+$  binding energies as a function of atomic number for  $1s_{1/2}$  configuration computed with  $U_Y = -30\text{MeV}$  (solid line) and  $-20\text{MeV}$  (dashed line).

**Table 2. Hyperon single-particle energies (in MeV) in core nucleus  $^{90}\text{Zr}$ .**

	$^{89}\Lambda\text{Y}(\text{exp})$	$^{91}\Lambda\text{Zr}$	$^{91}\Lambda_c^+\text{Nb}$			$^{91}\Lambda_b^+\text{Zr}$			
			-40	-30	-20	-40	-30	-20	-10
$1s_{1/2}$	-22.1	-22.4	-21.7	-11.5	-1.9	-34.2	-23.5	-13.6	-5.5
$1p_{3/2}$	-16.0	-16.3	-18.6	-8.9	-0.1	-31.1	-21.0	-11.8	-4.4
$1p_{1/2}$	(1p)	-16.2	-18.5	-8.8		-31.1	-21.0	-11.8	-4.4
$1d_{5/2}$	-9.5	-9.6	-14.6	-5.5		-27.9	-18.3	-9.8	-2.9
$2s_{1/2}$		-7.6	-12.2	-3.2		-27.0	-17.5	-9.1	-2.0
$1d_{3/2}$	(1d)	-9.4	-14.4	-5.3		-27.9	-18.3	-9.8	-2.9
$1f_{7/2}$	-2.5	-2.7	-10.0	-1.6		-24.6	-15.5	-7.7	-1.2

**Table 3. Hyperon single-particle energies(in MeV) in core nucleus  $^{208}\text{Pb}$ .**

	$^{208}\Lambda\text{Pb}(\text{exp})$	$^{209}\Lambda\text{Pb}$	$^{209}\Lambda_c^+\text{Bi}$		$^{209}\Lambda_b\text{Pb}$			
			- 40	- 30	- 40	- 30	- 20	- 10
$1s_{1/2}$	- 26.5	- 24.7	- 15.1	- 5.4	- 36.9	- 26.5	- 13.1	- 5.1
$1p_{3/2}$	- 21.3	- 21.0	- 13.8	- 4.2	- 34.8	- 24.8	- 11.6	- 3.9
$1p_{1/2}$	(1p)	- 21.0	- 13.7	- 4.2	- 34.8	- 24.8	- 11.5	- 3.9
$1d_{5/2}$	- 17.0	- 16.5	- 11.7	- 2.4	- 32.8	- 23.0	- 9.9	- 2.5
$2s_{1/2}$		- 14.5	- 9.1		- 32.5	- 22.5	- 9.3	- 2.0
$1d_{3/2}$	(1d)	- 16.4	- 11.6	- 2.3	- 32.8	- 23.0	- 9.8	- 2.5
$1f_{7/2}$	- 12.0	- 11.4	- 9.1	- 0.2	- 30.7	- 21.1	- 8.1	- 1.2

correspond to  $U_{\Lambda_c^+} = -30\text{MeV}$  and  $-20\text{MeV}$ , respectively. From the figure, we can see that the binding energies of  $\Lambda_c^+$  decrease as the nuclei get heavier. When the atomic number exceeds 100,  $\Lambda_c^+$  cannot bind to the nuclei if  $U_{\Lambda_c^+} = -20\text{MeV}$ . This suggests that, it appears preferable to search for  $\Lambda_c^+$ -hypernuclei in the medium-heavy systems.

When a baryonic impurity (a baryon different from nucleons) is added to an ordinary nucleus, its static properties may be affected. In order to observe the universal effects of impurities in nuclear core, we make a unified RMF calculation. In this work, typical hypernuclei between  $^7\text{Li}$  and  $^{209}\text{Pb}$  are selected, where  $Y = \Lambda, \Xi^-, \Xi^0, \Lambda_c^+, \Lambda_b, \Xi_c^+$  or  $\Xi_c^0$ .

Dover and Gal<sup>[25]</sup> analyzed the old emulsion data on  $\Xi^-$  hypernuclei, concluded a nuclear potential well depth of  $U_{\Xi} = -21 - -24\text{MeV}$ . Fukuda et al.<sup>[26]</sup> fitted to very low energy part of  $\Xi^-$  hypernuclear spectrum data in  $^{12}\text{C}(\text{K}^-, \text{K}^+)X$  reaction in experiments E224 at KEK, estimated the value of

$U_{\Xi}$  between  $-16$  and  $-20\text{MeV}$ . Recently, E885 at AGS<sup>[27]</sup> indicated a potential depth of  $U_{\Xi} = -14\text{MeV}$  or less. Here we choose  $U_{\Xi^-} = U_{\Xi^0} = -14\text{MeV}$  to determine  $g_{\sigma\Xi}$ . The results of  $\Lambda_c^+$  and  $\Lambda_b$  single-particle energies in Ref. [16] are very close to the corresponding result with  $U_{\Lambda} = -30\text{MeV}$ , so we adopt  $U_{\Lambda_c^+} = U_{\Lambda_b} = -30\text{MeV}$ . In addition, our calculations show that  $\Xi_c^+$ -hypernuclei are very unlikely to be formed if  $|U_{\Xi_c^+}| \leq 14\text{MeV}$ , so  $U_{\Xi_c^0} = U_{\Xi_c^+} = -16\text{MeV}$  is adopted here, making reference to the experimental data of  $\Xi$  hypernuclei.

The calculated results of  $\Lambda, \Xi^-$  and  $\Xi^0$  hypernuclei are shown in Table 4, results of ordinary nuclei are also given for comparison.  $-E/A$  is the binding energies (in MeV) per baryon,  $r_{\text{ch}}$  is the r.m.s. charge radius, and  $r_{\Lambda}, r_n$  and  $r_p$  are calculated r.m.s. radii (in fm) of  $\Lambda$  hyperon, neutron and proton distributions, respectively. All the hyperons are at their  $1s_{1/2}$  configuration in the hypernuclei. It can be found

**Table 4. Binding energy per baryon(in MeV), and r.m.s. radii of baryons(in fm).**

$^AZ$	$-E/A$	$r_{\text{ch}}$	$r_y$	$r_n$	$r_p$	$^AZ$	$-E/A$	$r_{\text{ch}}$	$r_y$	$r_n$	$r_p$
$^6\text{Li}$	5.67	2.52		2.32	2.37	$^{16}\text{O}$	8.04	2.70		2.55	2.58
$^7_{\Lambda}\text{Li}$	5.63	2.43	2.49	2.25	2.29	$^{17}_{\Lambda}\text{O}$	8.33	2.71	2.45	2.55	2.58
$^7_{\Xi^-}\text{Li}$	5.02	2.43	3.85	2.35	2.28	$^{17}_{\Xi^-}\text{O}$	7.98	2.68	2.89	2.57	2.55
$^7_{\Xi^0}\text{Li}$	4.86	2.55	4.43	2.27	2.41	$^{17}_{\Xi^0}\text{O}$	7.77	2.73	3.11	2.54	2.60
$^8\text{Be}$	5.42	2.48		2.30	2.34	$^{40}\text{Ca}$	8.52	3.46		3.31	3.36
$^9_{\Lambda}\text{Be}$	5.72	2.44	2.35	2.28	2.30	$^{41}_{\Lambda}\text{Ca}$	8.77	3.46	2.77	3.31	3.36
$^9_{\Xi^-}\text{Be}$	5.12	2.43	3.29	2.33	2.28	$^{41}_{\Xi^-}\text{Ca}$	8.67	3.44	2.95	3.33	3.34
$^9_{\Xi^0}\text{Be}$	4.93	2.50	3.69	2.27	2.36	$^{41}_{\Xi^0}\text{Ca}$	8.48	3.47	3.13	3.30	3.38
$^{12}\text{C}$	7.47	2.46		2.30	2.32	$^{208}\text{Pb}$	7.90	5.51		5.71	5.45
$^{13}_{\Lambda}\text{C}$	7.90	2.45	2.18	2.28	2.31	$^{209}_{\Lambda}\text{Pb}$	7.99	5.51	4.13	5.71	5.45
$^{13}_{\Xi^-}\text{C}$	7.34	2.43	2.80	2.32	2.29	$^{209}_{\Xi^-}\text{Pb}$	7.99	5.50	3.76	5.72	5.44
$^{13}_{\Xi^0}\text{C}$	7.12	2.48	3.05	2.27	2.34	$^{209}_{\Xi^0}\text{Pb}$	7.94	5.51	4.17	5.70	5.45

**Table 5. Binding energy per baryon(in MeV), and r. m. s. radii of baryons(in fm), with the contribution of  $\rho$  meson fields.**

${}^AZ$	$-E/A$	$r_{ch}$	$r_y$	$r_n$	$r_p$	${}^AZ$	$-E/A$	$r_{ch}$	$r_y$	$r_n$	$r_p$
${}^6\text{Li}$	5.67	2.52		2.32	2.37	${}^{16}\text{O}$	8.04	2.70		2.55	2.58
${}^7_{\Lambda_c^+}\text{Li}$	5.99	2.42	1.88	2.23	2.28	${}^{17}_{\Lambda_c^+}\text{O}$	8.33	2.72	2.04	2.56	2.59
${}^7_{\Lambda_b}\text{Li}$	7.04	2.37	1.39	2.19	2.22	${}^{17}_{\Lambda_b}\text{O}$	8.87	2.71	1.57	2.56	2.58
${}^7_{\Xi_c^+}\text{Li}$	5.17	2.38	2.59	2.37	2.24	${}^{17}_{\Xi_c^+}\text{O}$	7.97	2.68	2.39	2.58	2.55
${}^7_{\Xi_c^0}\text{Li}$	4.90	2.59	2.97	2.22	2.46	${}^{17}_{\Xi_c^0}\text{O}$	7.71	2.74	2.55	2.53	2.61
${}^8\text{Be}$	5.42	2.48		2.30	2.34	${}^{40}\text{Ca}$	8.52	3.46		3.31	3.36
${}^9_{\Lambda_c^+}\text{Be}$	6.00	2.43	1.79	2.25	2.29	${}^{41}_{\Lambda_c^+}\text{Ca}$	8.64	3.47	2.48	3.32	3.37
${}^9_{\Lambda_b}\text{Be}$	6.99	2.38	1.28	2.21	2.23	${}^{41}_{\Lambda_b}\text{Ca}$	8.94	3.46	1.94	3.32	3.36
${}^9_{\Xi_c^+}\text{Be}$	5.24	2.40	2.38	2.34	2.26	${}^{41}_{\Xi_c^+}\text{Ca}$	8.56	3.44	2.70	3.33	3.34
${}^9_{\Xi_c^0}\text{Be}$	4.96	2.53	2.61	2.24	2.39	${}^{41}_{\Xi_c^0}\text{Ca}$	8.35	3.48	2.89	3.30	3.38
${}^{12}\text{C}$	7.47	2.46		2.30	2.32	${}^{208}\text{Pb}$	7.90	5.51		5.71	5.45
${}^{13}_{\Lambda_c^+}\text{C}$	8.13	2.43	1.59	2.26	2.29	${}^{209}_{\Lambda_c^+}\text{Pb}$	7.89	5.51	4.65	5.71	5.45
${}^{13}_{\Lambda_b}\text{C}$	7.90	2.44	2.13	2.28	2.30	${}^{209}_{\Lambda_b}\text{Pb}$	7.99	5.51	3.64	5.71	5.45
${}^{13}_{\Xi_c^+}\text{C}$	7.42	2.41	2.13	2.33	2.27	${}^{209}_{\Xi_c^+}\text{Pb}$	7.90	5.50	4.26	5.72	5.44
${}^{13}_{\Xi_c^0}\text{C}$	7.13	2.49	2.29	2.26	2.35	${}^{209}_{\Xi_c^0}\text{Pb}$	–	–	–	–	–

**Table 6. Binding energy per baryon(in MeV), and r. m. s. radii of baryons(in fm), without the contribution of  $\rho$  meson fields.**

${}^AZ$	$-E/A$	$r_{ch}$	$r_y$	$r_n$	$r_p$	${}^AZ$	$-E/A$	$r_{ch}$	$r_y$	$r_n$	$r_p$
${}^6\text{Li}$	5.67	2.52		2.32	2.37	${}^{16}\text{O}$	8.04	2.70		2.55	2.58
${}^7_{\Xi^-}\text{Li}$	5.08	2.47	3.37	2.29	2.33	${}^{17}_{\Xi^-}\text{O}$	8.02	2.70	2.73	2.55	2.58
${}^7_{\Xi^0}\text{Li}$	4.89	2.49	3.82	2.30	2.35	${}^{17}_{\Xi^0}\text{O}$	7.79	2.71	2.98	2.55	2.58
${}^7_{\Xi_c^+}\text{Li}$	5.32	2.45	2.21	2.27	2.31	${}^{17}_{\Xi_c^+}\text{O}$	8.03	2.71	2.20	2.55	2.58
${}^7_{\Xi_c^0}\text{Li}$	5.00	2.48	2.45	2.28	2.34	${}^{17}_{\Xi_c^0}\text{O}$	7.74	2.71	2.41	2.55	2.58
${}^8\text{Be}$	5.42	2.48		2.30	2.34	${}^{40}\text{Ca}$	8.52	3.46		3.31	3.36
${}^9_{\Xi^-}\text{Be}$	5.18	2.46	2.96	2.29	2.32	${}^{41}_{\Xi^-}\text{Ca}$	8.69	3.46	2.83	3.31	3.36
${}^9_{\Xi^0}\text{Be}$	4.97	2.47	3.29	2.30	2.33	${}^{41}_{\Xi^0}\text{Ca}$	8.48	3.46	3.12	3.31	3.36
${}^9_{\Xi_c^+}\text{Be}$	5.37	2.45	2.07	2.28	2.31	${}^{41}_{\Xi_c^+}\text{Ca}$	8.58	3.46	2.52	3.31	3.36
${}^9_{\Xi_c^0}\text{Be}$	5.05	2.46	2.27	2.28	2.32	${}^{41}_{\Xi_c^0}\text{Ca}$	8.35	3.46	2.87	3.31	3.36
${}^{12}\text{C}$	7.47	2.46		2.30	2.32	${}^{208}\text{Pb}$	7.90	5.51		5.71	5.45
${}^{13}_{\Xi^-}\text{C}$	7.40	2.45	2.58	2.29	2.31	${}^{209}_{\Xi^-}\text{Pb}$	7.98	5.51	4.83	5.71	5.44
${}^{13}_{\Xi^0}\text{C}$	7.16	2.46	2.82	2.29	2.32	${}^{209}_{\Xi^0}\text{Pb}$	7.92	5.51	4.34	5.71	5.45
${}^{13}_{\Xi_c^+}\text{C}$	7.54	2.44	1.87	2.28	2.30	${}^{209}_{\Xi_c^+}\text{Pb}$	7.93	5.51	3.94	5.71	5.45
${}^{13}_{\Xi_c^0}\text{C}$	7.20	2.45	2.04	2.29	2.31	${}^{209}_{\Xi_c^0}\text{Pb}$	–	–	–	–	–

that, for lighter  $\Lambda$ -hypernucleus, size of the core nucleus in a hypernucleus is smaller than the one in free space, i. e., both the values of  $r_n$  and  $r_p$  get smaller in hypernucleus. Although there are only a bit of shrinkage in the core nucleus due to the presence of  $\Lambda$  impurity, the glue-like role of  $\Lambda$  is obtained, in agreement with KEK-PS E419 experiment. It can be seen from the table that the effect of  $\Lambda$  on nuclear core is gradually decreasing with increasing mass number. The

above RMF results have revealed the universality of the shrinkage effect in lighter  $\Lambda$  hypernuclei, however, situation of  $\Xi$  hypernuclei is quite different. By adding a  $\Xi^-$  hyperon into nuclei, the r. m. s. radii of neutrons become a little larger, while those of protons become much smaller; Contrary to the  $\Xi^-$  hypernuclei, adding a  $\Xi^0$  hyperon will cause the proton r. m. s. radii to become larger, and the neutron ones to become smaller. Obviously that the common explanation<sup>[28]</sup>

for the shrinkage does not suit the case of  $\Xi^-$  and  $\Xi^0$  now. Both  $\Lambda$  and  $\Xi^0$  hyperon are neutral, hence the origin of the above difference cannot be owed to their Coulomb potential.

To see the effects of heavy flavored baryons impurities on nuclear core, results of  $\Lambda_c^+$ ,  $\Lambda_b$ ,  $\Xi_c^0$  and  $\Xi_c^+$  hypernuclei are shown in Table 5, results of ordinary nuclei are also given. We can see that both  $r_n$  and  $r_p$  become smaller when a  $\Lambda_c^+$  or  $\Lambda_b$  is added to a lighter nucleus. That is to say these two hyperons play the glue-like role in lighter nuclei. But, for other heavier nuclei, such as  $^{17}\text{O}$ ,  $r_n$  and  $r_p$  become a little larger than that in ordinary nuclei. While a  $\Xi_c^0$  is added to a nucleus, the situation is the same as a  $\Xi^-$  hyperon; The effects of  $\Xi_c^+$  is the same as of a  $\Xi^0$ .

Different behavior of  $\Lambda$  ( $\Lambda_c^+$ ,  $\Lambda_b$ ),  $\Xi^-$  ( $\Xi_c^0$ ) and  $\Xi^0$  ( $\Xi_c^+$ ) in-nuclear impurities is believed to come from the differences of their third isospin component, which couples with the  $\rho$  meson fields in RMF model. After eliminating contributions of the  $\rho$  mesons, the RMF results are shown in Table 6. Now we find that both the r. m. s. radii of protons and neutrons reduce when adding a  $\Xi^-$  ( $\Xi_c^0$ ) or  $\Xi^0$  ( $\Xi_c^+$ ) hyperon to the nuclei, the same as the situation of adding a  $\Lambda$  hyperon. It is also seen that, the effects of heavy flavored baryons on heavier nuclei is very little.

If the contribution of  $\rho$  mesons is ignored, we obtain the same nuclear shrinkage by adding a  $\Xi^-$  ( $\Xi_c^0$ ) or  $\Xi^0$  ( $\Xi_c^+$ ) to lighter nuclei. So we can conclude that, the  $\rho$  meson field plays an important role, and the different behavior of the  $\Lambda$  ( $\Lambda_c^+$ ,  $\Lambda_b$ ),  $\Xi^-$  ( $\Xi_c^0$ ) and  $\Xi^0$  ( $\Xi_c^+$ ) impurities is due to

their different third component of isospin.

## 4 Summary and conclusions

Within the framework of the RMF model, we have performed comprehensive calculations of three kind of flavored nuclei (strange, charmed and bottom hypernuclei), using consistent force parameters NL-SH for the nucleonic sector. The potential well depths and coupling constants of these flavored baryons are estimated and the results show rich and colorful behavior.

The effects of different baryons impurities on the core nucleus are also examined. It is shown that for lighter  $\Lambda$  hypernuclei, unlike the conclusion of Ref. [29], the glue-like role of the  $\Lambda$  impurity is universal— $\Lambda$  has the same effects on the core proton distribution and the neutron one. Our results of heavy flavored hypernuclei show that both hyperons  $\Lambda_c^+$  and  $\Lambda_b$  play the glue-like role as  $\Lambda$  does in lighter hypernuclei; but the effects of  $\Xi$  or  $\Xi_c$  hyperon on the core nucleus are different. The results suggest that, for  $\Xi^-$  or  $\Xi_c^0$  hypernuclei, the proton distribution has a little shrinkage effect, whereas the neutron distribution shows a little swell. For  $\Xi^0$  or  $\Xi_c^+$  hypernuclei the trend of the variety is contrary to the above.

Although our results for charmed and bottom hypernuclei should be regarded as a qualitative estimate, they may exhibit some general features that may remain valid after we learn more about the interaction between flavored baryon and nucleon.

## References

- 1 Millener D J, Dover C B, Gal A. Phys. Rev., 1988, **C38**: 2700
- 2 Halderson D. Phys. Rev., 1993, **C48**: 581; 2000, **C61**: 034001
- 3 Gal A. Nucl. Phys., 2000, **A670**: 229c
- 4 Noumi H et al. Phys. Rev. Lett., 2002, **89**:072301
- 5 Dover C B, Kahana S H. Phys. Rev. Lett., 1977, **39**: 1506
- 6 Bando H, Nagata S. Prog. Theor. Phys., 1983, **69**: 557
- 7 Bando H, Bando M. Phys. Lett., 1982, **B109**: 164
- 8 Batusov Y A et al. Sov. J. JETP Lett., 1981, **33**: 56
- 9 Bressani T, Iazzi F. Nuo. Cim., 1989, **A102**: 597
- 10 Buyatov S A et al. Nuo. Cim., 1991, **A104**: 1361
- 11 Serot B D, Walecka J D. Adv. Nucl. Phys., 1986, **16**: 1
- 12 Sharma M M, Nagarajan M A, Ring P. Phys. Lett., 1993, **B312**: 377
- 13 MA Z Y, Speth J, Krewald S et al. Nucl. Phys., 1996, **A608**:305
- 14 Ring P. Prog. Part. Nucl. Phys., 1996, **37**: 193
- 15 TAN Y H, SHEN H, NING P Z. Phys. Rev., 2001, **C63**: 055203
- 16 Tsushima K, Khanna F C. Phys. Rev., 2003, **C67**: 015211
- 17 Glendenning N K, Moszkowski S A. Phys. Rev. Lett., 1991, **67**:2414
- 18 Schaffner J, Greiner C, Stöcker H. Phys. Rev., 1992, **C46**: 322
- 19 TAN Y H, LUO Y A, NING P Z et al. Chin. Phys. Lett., 2001, **18**: 1030
- 20 Starkov N I, Tsarev V A. Nucl. Phys., 1986, **A450**: 507c
- 21 Rufa M et al. Phys. Rev., 1990, **C42**: 2469
- 22 Shen H, Toki H. Nucl. Phys., 2002, **A707**: 469
- 23 Ajimura S et al. Nucl. Phys., 1995, **A585**: 173
- 24 Usmani Q N, Bodmer A R. Phys. Rev., 1999, **C60**: 055215
- 25 Dover C B, Gal A. Ann. Phys (NY), 1983, **146**: 309
- 26 Fukuda F et al. Phys. Rev., 1998, **C58**: 1306
- 27 Khaustov P et al. Phys. Rev., 2000, **C61**: 054603
- 28 Tanida K, Tamura H, Abe D et al. Phys. Rev. Lett., 2001, **86**: 1982
- 29 Tsushima K, Saito K, Thomas A W. Phys. Lett., 1997, **B411**: 9

## 超核的相对论平均场计算<sup>\*</sup>

宁平治<sup>1)</sup> 谭玉红 李磊 罗延安

(南开大学物理系 天津 300071)

**摘要** 利用相对论平均场方法计算了奇异、粲和底超核的部分性质,包括各种不同味的超核的单粒子能量以及其他一些静态性质,并对结果进行了比较.对各种味的重子的势阱深度和耦合常数做了估计,得到丰富的结果.建议寻找质量数大于 100 的粲超核.同时探讨了不同重子杂质对原子核芯性质的可能影响.

**关键词** 不同味的原子核 重味重子-核势 单粒子谱 相对论平均场方法

---

Received 29 November 2003, Revised 29 March 2004

<sup>\*</sup> 国家自然科学基金(10275037)和国家教育部博士点专项基金(20010055012)资助

1) E-mail: ningpz@nankai.edu.cn